Myocardial CT perfusion imaging for ischemia detection

Patricia Carrascosa, Carlos Capunay

Department of Cardiovascular Imaging, Diagnóstico Maipú, Buenos Aires, Argentina

Contributions: (I) Concept and design: All authors; (II) Administrative support: All authors; (III) Provision of study material or patients: All authors; (IV) Collection and assembly of data: All authors; (V) Data analysis and interpretation: All authors; (VI) Manuscript and interpretation: All authors; (VII) Manuscript writing: All authors.

Correspondence to: Patricia Carrascosa, MD, PhD, FSCCT. Av Maipú 1668, Vicente López (B1602ABQ), Buenos Aires, Argentina. Email: patriciacarrascosa@diagnosticomaipu.com.ar.

Abstract: Coronary computed tomography angiography (CCTA) plays an important role in many specific scenarios such as in symptomatic patients with intermediate pretest of coronary artery disease (CAD), as well as in the triage of patients with acute chest pain with TIMI risk ≤2. However, it cannot detect the presence of associated ischemia, which is critical for clinical decision making among patients with moderate to severe stenosis. Although functional information can be obtained with different noninvasive tools, cardiac CT is the unique modality that can perform a comprehensive evaluation of coronary anatomy plus the functional significance of lesions. Myocardial CT perfusion (CTP) can be performed with different approaches such as static and dynamic CTP. In addition, static CTP can be performed using single energy CT (SECT) or dual energy CT (DECT). In this review, we will discuss the technical parameters and the available clinical evidence of static CTP using both SECT and DECT.

Keywords: Computed tomography (CT); perfusion defect; necrosis; dipyridamole; dual energy imaging

Introduction

Computed tomography (CT) has evolved significantly during the last two decades mainly with the introduction of multidetector CT (MDCT) in 1998 (1-3). Since the first 4-row MDCT scanners until now this technology has upgraded significantly in contrast, spatial, and temporal resolutions. Current MDCT scanners can perform accurate noninvasive assessment of the coronary arteries by means of coronary computed tomography angiography (CCTA), which plays an important role in many specific scenarios such as in symptomatic patients with intermediate pretest of coronary artery disease (CAD), as well as in patients with acute chest pain with TIMI risk ≤2, among others. In the setting of suspected stable CAD, large multicenter trials such as the PROMISE (4) and SCOT-HEART (5) have demonstrated that CCTA is clinically useful as an alternative or in addition to functional testing. In the triage of patients with acute chest pain, also large trials such as CT-STAT (6), ACRIN-

PA (7), ROMICAT II (8), CT-COMPARE (9) and real world scenario (10,11) in where CCTA was rivaled with standard of care, have demonstrated that negative CT findings allowed to safety rule out CAD and identify patients eligible for early discharge from the emergency department.

CCTA has a very high negative predictive value to rule out CAD, and during the last decade the positive predictive value has raised to achieve current values of nearly 80% (12-14). CCTA has the ability to evaluate the lumen as well as the vessel wall, thereby having the ability to characterize the atherosclerotic plaques that are generating stenosis (15-17). In the past year, a reporting and data system document known as Coronary Artery Disease Reporting and Data System (CAD-RADS™) (18) was published, aimed to standardize the communication of CCTA findings in order to facilitate decision-making according to the results that helps for further management. In relation to the degree of coronary stenosis obstruction,

a scale is divided in 6 grades. In the cases where moderate or moderate to severe stenosis are present, a functional assessment is recommended as clinical decision is related to the functional impact that the coronary stenosis is producing. Documentation of the extension and severity of ischemia is required to establish the need for invasive versus medical management of CAD. Different diagnostic tools can perform such functional evaluation, including single photon emission computed tomography (SPECT) (19-22), stress-cardiovascular magnetic resonance (CMR) (23-27), stress echocardiography (28-30) and positron emission tomography (PET) (31). Although the functional information provided by any of them is extremely useful regarding therapeutic decisions and prognosis, none of them can perform a comprehensive anatomical-functional evaluation within the same study. For that reason, myocardial CT Perfusion (CTP) was born with the potential to accomplish such analysis.

The first myocardial CTP studies started two decades ago using electron beam CT, achieving quantitative myocardial perfusion imaging with promising results (32). Nonetheless, only one decade ago, the development of myocardial CTP using multidetector CT became feasible (33).

Many single and multicenter studies have validated the results of myocardial CTP against other modalities such as SPECT, CMR, PET, invasive coronary angiography (ICA) and invasive fractional flow reserve (FFR) (34-42). Most of these were performed in a limited number of patients and using different scanner generations, showing high sensitivity and negative predictive value, and moderate specificity and positive predictive value. Newer single center studies have shown improved positive predictive value as well as specificity, being validated by two large multicenter trials (43-46).

Myocardial CTP imaging may be performed only at rest or with pharmacologic stress. There are two main methods for CTP acquisition: static and dynamic myocardial CTP. Static myocardial CTP, which has been more extensively investigated, obtains myocardial perfusion at a specific timepoint during iodinated contrast injection. It enables a qualitative and/or semi-quantitative assessment of myocardial CTP. In contrast, dynamic myocardial CTP imaging consists in uninterrupted imaging of myocardial perfusion, as iodinated contrast passages from the aorta and coronary arteries and throughout the myocardium. It therefore allows a qualitative, semi-quantitative, and/or quantitative assessment of myocardial perfusion.

In any of the modes, iodinated contrast attenuates X-rays proportionally to the concentration of iodine, therefore hypoattenuated areas in the myocardium on CT images represent myocardial regions of hypoperfusion and/or reduced intravascular blood volume.

Rest-only myocardial CTP application is very limited, since it can detect (rest) ischemia mainly in cases where very severe stenosis is present. For that reason, the majority of the patients demand a pharmacologic stress scan to determine the presence or absence of functional relevance of a coronary stenosis, that generally require a minimum of 50% stenosis to be able to reduce hyperemic myocardial blood flow (47).

In this review, we will focus exclusively in static myocardial CTP. Static myocardial CTP, also known as first pass CTP, consists in a dual CT scan in stress and rest that can be acquired with single energy CT (SECT) or dual energy CT (DECT).

Single energy myocardial CTP

Two CT scans have to be carried out: one with pharmacological stress and another in rest. The decision to select the opening scan depends on the pre-test of the patient and/or the extent of calcium score. It is better to start with the stress phase among patients with intermediate to high pre-test and with moderate to high calcium scores, as ischemia needs to be prioritized. When stress CT imaging is performed first, the myocardium is not contaminated by any previous contrast media. On the other hand, it is preferred to initiate with the rest phase if the patient has low to intermediate probability of CAD with no calcium or mild calcium in the coronary arteries, as it is highly probable that the patient has normal coronary arteries, and the high negative predictive value of the CCTA will allow to rule out CAD and thus won't require to continue with the stress phase.

In case where rest CT scan is performed first and a coronary artery stenosis is detected, only if the stenosis is over 40–50% it might be necessary to complement with a stress scan to evaluate the functional relevance. On the other hand, if a severe coronary stenosis >90% is detected, no stress CT scan needs to be done as it is highly likely that this coronary stenosis is associated with myocardial ischemia (48).

It is suggested that at least 10 minutes must separate the two CT scans to avoid contrast agent contamination of the myocardium and in situations of hypo-perfusion areas in the stress scans, to enable normalization of myocardial perfusion (*Figure 1*) (37).
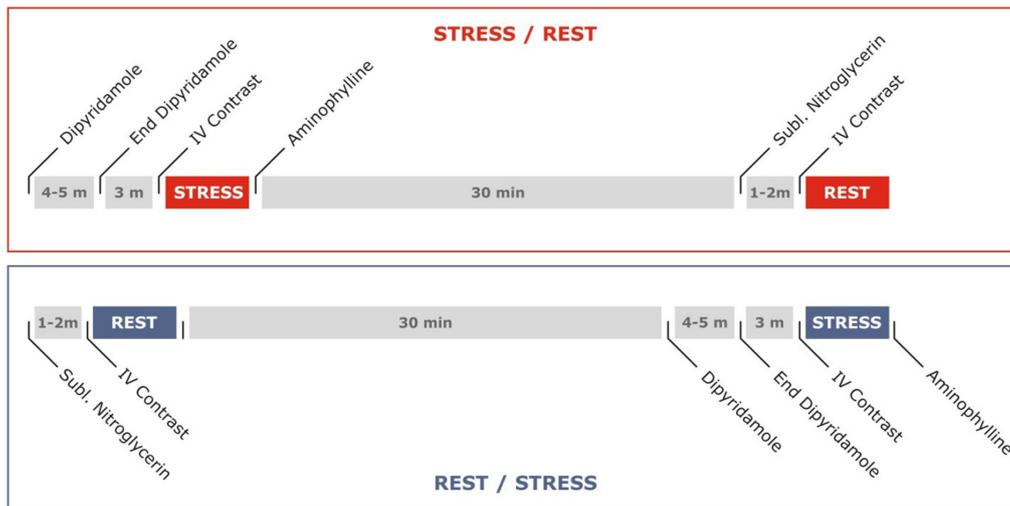
Figure 1 Example of a myocardial CT perfusion protocol.

Stress phase CT scan

Stress CT scan is acquired using retrospective ECG-gating with tube current modulation in order to reduce radiation dose and have the possibility to analyze systolic and diastolic phases to distinguish motion artifacts from true myocardial perfusion defects. A true myocardial perfusion defect has to be identified in both phases of the cardiac cycle.

Stress myocardial CTP imaging requires the administration of vasodilator stress agents. There are currently three drugs commonly used for myocardial CTP: adenosine, dipyridamole, and regadenoson (49-55). In any case, two intravenous (IV) lines are essential for CTP studies: one for contrast injection and another for administration of the vasodilator agent. There are differences among the vasodilators in terms of mechanism of action, half-life and way of infusion.

Adenosine is a non-specific adenosine receptor agonist, with a half-life of only 10 seconds that demands a continuous infusion via an IV pump. It is associated with low rate of adverse effects. In the Core 320 study, a 0.4% incidence of transient heart block and 0.2% of hypotension has been reported (56).

Dipyridamole is an adenosine deaminase and phosphodiesterase inhibitor that causes vasodilation of normal coronary arteries via the accumulation of endogenous adenosine. It has a longer half-life than adenosine, of approximately 30 minutes (disadvantage), and therefore demands turnaround with aminophylline. It does not require

an IV pump for infusion as it can be applied manually at a slow rate in a period of 4 minutes. After administration of 0.56 mg/kg, images have to be acquired during the following 3 minutes. The main advantage of this drug is the low cost. Two IV lines are preferred instead of one because dipyridamole can irritate the vessel wall. To revert the effect of dipyridamole, 1 mg/kg of aminophylline is administrated in 30–60 s dispensed via an IV line. In cases of persistent symptoms or ECG changes, dose can be complemented up to 250 mg (57).

Regadenoson is a specific A2A adenosine receptor agonist. It does not require an IV pump, as it is administered via a prefilled syringe over 10 seconds. It is a safer option for patients with bronchospastic lung disease. However, it is more expensive than adenosine and dipyridamole and it is not widely available.

Rest phase as second CT scan

The rest CT scan is performed after the stress CT scan if myocardial ischemia wants to be prioritized. This acquisition is usually carried out using a prospectively ECG-triggered CT scan protocol to reduce radiation dose. In many patients, after reverting the effect of the vasodilator the heart rate returns to basal; although in some patients there is persistence of elevated heart rate. If the patient has a heart rate <65 bpm, prospective CT scan centered at 75% of the R-R interval is generally used. Additional padding can be complemented (82–100 ms) especially in cases where patients after

cdt.amegroups.com   *Cardiovasc Diagn Ther* 2017;7(2):112-128
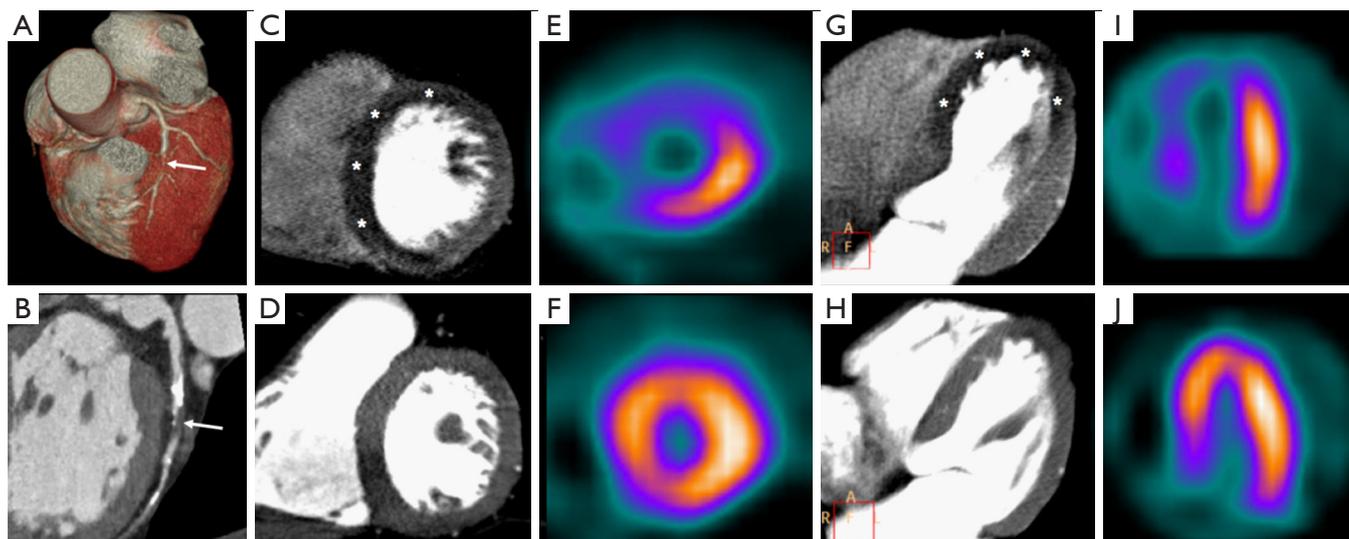
Figure 2 Single energy static CT myocardial perfusion. A 61-year-old male, with stable angina. Body mass index 31 kg/m^2. Cardiovascular risk factors: hypercholesterolemia, former smoker. (A) Volume rendering of the heart: a severe stenosis (arrow) is observed at the mid left anterior descending artery (LAD); (B) curved multiplanar reconstruction of the LAD: there are proximal calcified plaques and there is a mixed, predominately non-calcified plaque at the mid-portion generating a severe stenosis (arrow); (C) stress short axis CT: large and severe hypoperfusion is observed at the septal, anterior, antero-septal and infero-septal walls (*); (D) rest short axis CT: normal myocardial perfusion demonstrating that the defects observed in stress correspond to ischemia; (E,F) short axis SPECT at stress and rest showing same findings than CT; (G) stress four chamber CT: severe hypo-perfusion is observed at the apical and septal wall (*); (H) rest four chamber CT: normal myocardial perfusion; (I,J) stress-rest four chamber SPECT images showing similar results.

the stress scan persist with higher heart rate. However, padding is associated with higher radiation dose.

In this phase it is necessary to accurately evaluate the coronary arteries to diagnose or rule out the presence of CAD as well as characterize the eventual plaque/plaques. Furthermore, is important to see if there is any myocardial perfusion defect associated.

There are different behaviors of the myocardial perfusion defects in stress and rest CT scans:

(I) Hypoperfusion in stress with normal perfusion in rest: Ischemia (*Figure 2*);

(II) Hypoperfusion in stress that persists with same extension in rest: Necrosis;

(III) Hypoperfusion in stress that persists in rest with less extension than in stress: Peri-necrosis ischemia;

(IV) Normal myocardial perfusion at stress and rest CT scans.

Rest phase as the first CT scan

When the rest CT scan is the first acquisition, patients with high heart rate commonly receive beta-blockers to reduce

heart rate and enable performing a prospective ECG-gated CT scan. If heart rate is low, prospective ECG triggered CT scan, centered at 75% phase of the R-R cycle can be carried out without padding.

Myocardial perfusion defects can be observed during the rest phase only in cases of severe coronary artery stenosis (>90%) or in cases of acute obstructions. Also myocardial perfusion defects associated with necrosis can be identified, although in this review we will only cover reversible defects.

When a moderate coronary artery stenosis is present, a complementary stress CT acquisition can be performed in order to determine the clinical relevance of that stenosis. If no stenosis or mild coronary artery stenosis is detected, the study does not require to be complemented with a stress scan, thus avoiding further radiation and iodinated contrast exposure.

Contrast agent

For both rest and stress CT scans, intravenous contrast agent has to be applied using a power injector. The contrast volume is related to the patient´s weight and

the type of scanner used, ranging from 60–120 mL in SECT scanners. It can be significantly reduced if DECT technique is applied. The contrast bolus should be delivered with a total injection time of 10 s or less. It is recommended to inject a saline chaser (40–50 mL) following the iodine contrast bolus. Contrast can be heated to 37 degrees Celsius (98.6 degrees Fahrenheit) to improve viscosity and obtain better contrast injection. It is recommended to explain patients about the common sensations the iodine contrast agent may cause in order to avoid any patient motions, whether breathing or body movements, during the scan. There are two manners of contrast injection: (I) Bolus Timing scan (BTS) which allows to calculate the bolus transit time to determine when to initiate the contrast injection and when to scan. A graph is given combining Hounsfield Units and time. The graph provides the user with tick marks visualized in the graphic that represents how the contrast is enhancing the vessels and its washout. Counting from the first tick mark up to the one with highest HU, the number of marks multiplied by 2 and adding 5 s for scan preparation delay provides the exact time to start the CT acquisition; (II) Smart Prep (SM) or automatic bolus tracking system helps to synchronize the acquisition with the contrast injection. Once the predefined threshold is reached at the desire localization, the CT scan is triggered and the complete examination is performed.

Scan delay

CTP imaging has to be done during the early first-pass of the contrast, when the iodine contrast is mainly intravascular. The test-bolus or the bolus-tracking are the two available techniques for CT timing.

Technical parameters

Both tube voltage and current have to be set according to the patient's body mass index (BMI). In patients with BMI <30, tube voltage is adjusted to 100 kV and tube current between 270–320 mAs (prospective acquisitions) or 800 mAs (retrospective scans), while in patients with BMI >30, tube voltage is adjusted to 120 kV and tube current between 370–450 mAs (prospective acquisitions) or 1,000 mAs (retrospective scans). In obese patients with BMI >40, tube voltage can be set at 140 kV and tube current up to 500–600 mAs (prospective acquisitions) or 1,200 mAs (retrospective scans).

Use of nitroglycerin

Nitroglycerin is used before the rest CT scan to dilate the coronary arteries and improve coronary artery visualization. It cannot be administered in conjunction with the stress drug in order to avoid severe hypotension. It is recommended to wait 20 minutes between the administration of short-acting, sublingual nitroglycerin and vasodilator stress agents (57).

Iterative reconstruction (IR)

IR was introduced in the last years. This image reconstruction algorithm allows a significant improvement in image quality, thus enabling the achievement of similar image quality at reduced radiation doses. In this way a stress-rest or rest-stress myocardial CTP can be done with less than 9 mSv, achieving similar radiation doses than a SPECT scan (58,59).

Limitations

A main challenge of myocardial CTP are beam hardening artifacts (BHA) (60). These artifacts arise from the polychromatic nature of the X-rays in the CT acquisitions and the presence of high contrast density in the heart chambers. BHA are associated with non-uniform changes in CT densitometry in the myocardium that generates false perfusion defects. With the development of DECT, BHA can be attenuated or even cancelled by the generation of monochromatic images at medium to high energy levels.

Clinical evidence

A large number of clinical studies have explored the diagnostic performance of myocardial CTP, showing a good sensitivity and negative predictive value, with modest specificity and positive predictive value (34-37). Most of these were single center, had small sample size, and used different reference standard modalities including ICA, SPECT, CMR perfusion, and FFR. Furthermore, there are substantial differences regarding patient population and scanner generation, ranging from 16-slice CT to 320-slice and dual source CT scanners. Finally, additional methodological differences can be noted including image analysis, endpoints, and coronary territories (per patient, per vessel, per segment analyses).

Table 1 Studies assessing static myocardial CT perfusion using single energy CT

Study	Scanner	Acquisition	No. of patients	Patients	Radiation dose (mSv)[¶]	Sensitivity (%, per vessel)	Specificity (%, per vessel)
Kurata *et al.* (34)	16 detector	Retrospective	12	Suspected CAD	Not reported	90	79
George *et al.* (35)	64 & 256 detector	Retrospective	27	Positive SPECT	16.8 (64 CT) 21.6 (256 CT)[†]	81	85
Blankstein *et al.* (36)	64 DSCT	Retrospective	33	Recent SPECT and ICA	9.1	93	74
Rocha-Filho *et al.* (61)	64 DSCT	Retrospective	34	Recent SPECT and ICA	9.8	91	91
Tamarappoo *et al.* (38)	64 DSCT	Retrospective	30	Positive SPECT	15.7	92[‡]	86[‡]
Ko *et al.* (41)	320 detector	Prospective	42	Known CAD awaiting revascularization	5.3	76	84
Ko *et al.* (42)	320 detector	Prospective	40	Suspected CAD	4.5	95	95
Bettencourt *et al.* (43)	64 detector	Retrospective	101	Suspected CAD	5.0 (including rest CCTCA)	71	90
Rochitte *et al.* (56)	320 detector	Prospective	381	Suspected or knownCAD	9.3	80[£]	74[£]
Cury *et al.* (45)	Multivendor	Prospective	110	Suspected or knownCAD	N/A	90[µ]	84[µ]

*, No. of patients in the study who underwent both CTP and reference standard imaging modality. [¶], radiation dose only for the stress perfusion acquisition. [†], only the radiation dose for both stress and rest perfusion was reported. [‡], per segment has been reported. [£], assuming a summed stress score of 4. [µ], per patient results available only. N/A, not available.

Overall, most studies demonstrated high sensitivity and moderately high specificity, with a significant decline in effective radiation dose within the newest studies compared to the early experiences (*Table 1*). Importantly, several studies demonstrated that the evaluation of stress-CTP provides a significant incremental value over the mere assessment of coronary anatomy using CCTA alone.

George *et al.* were among the first to perform a semi-quantitative assessment of myocardial CTP using SECT (35). By means of a combined definition of ICA-derived stenosis ≥50% with a corresponding SPECT perfusion abnormality, in a pilot study, George *et al.* demonstrated that combined CCTA and CTP had a sensitivity, specificity, positive predictive value, and negative predictive value of 86%, 92%, 92%, and 85%, respectively. The semi-quantitative metric applied was the transmural perfusion ratio (TPR) (37).

Another small study conducted by Blankstein *et al.* performed adenosine stress CTP, rest CCTA, and a delayed CT scan using a first generation dual source CT scanner and ICA as reference standard (36). In this study, stress CTP showed good sensitivity and specificity for the detection of stress-induced myocardial perfusion defects, with the advantage of providing coronary anatomy data at comparable radiation dose (12.7 mSv both).

Later, the same authors demonstrated a significant incremental value of stress CTP over CCTA alone, with improvements in sensitivity (from 83% to 91%) and specificity (from 71% to 91%) for the detection of significant coronary stenosis (61).

Static myocardial CTP has also been compared against stress CMR perfusion. Using a high-pitch 128 slice dual-source CT protocol among 39 intermediate to high risk patients, Feuchtner *et al.* compared adenosine stress CTP with adenosine stress CMR. Stress CTP demonstrated high per-vessel sensitivity (96%) and specificity (88%) for the detection of perfusion defects, and also for the identification of reversible ischemia (sensitivity of 95% and specificity of 96%). Interestingly, stress CTP provided a significant incremental value over CCTA, with the diagnostic accuracy improving from 84% to 95%. Notably, the mean effective radiation dose was merely 2.5 mSv (39).

A number of studies have also explored the diagnostic performance of CTP using FFR as reference standard, showing similar results. In particular, two studies confirmed the improved diagnostic performance of the combined assessment of CTA and CTP using both 64

and 320 detector CT (41,61). Both studies suggested that the improved diagnostic performance was related to the improvement in the specificity and positive predictive value when added to CCTA alone.

One of the potentially useful applications of CTP is among patients with previous revascularization. In this regard, Rief *et al.* demonstrated in 92 patients that static CTP significantly improved the detection of in-stent restenosis (area under the curve from 0.69 to 0.92; P<0.0001) by reducing the number of non-diagnostic CTA examinations (62).

The aforementioned results from single center studies have been further validated in two large multicenter studies: the Core 320 (56) and the multivendor multicenter trial (45) using regadenoson. In the Core 320 study, Rochitte *et al.* (56) studied the diagnostic performance of combined CCTA and CTP using a 320 detector row scanner among 381 patients with suspected or known CAD. A positive finding was a coronary stenosis ≥50% by ICA associated with corresponding perfusion defect on SPECT. The combined anatomic and functional evaluation (CCTA + CTP) on a per patient basis showed an improvement in diagnostic performance from an AUC of 0.82 with CCTA alone to AUC 0.87 for combined evaluation (P<0.001).

Cury *et al.* (45) performed another multicenter trial using different vendor scanners (64, 128, 256 or 320 detector row). They enrolled 110 patients with suspected or known CAD, and also regadenoson was used as stress agent. The primary endpoint of non-inferiority compared to SPECT was achieved, with an agreement rate for detecting or excluding ≥1 fixed defects by regadenoson CTP and SPECT of 0.86 (95% CI, 0.74–0.98). In this study, the diagnostic accuracies of CTP and CCTA alone were 0.85 (95% CI, 0.78–0.91) and 0.69 (95% CI, 0.60–0.77), respectively.

Dual-energy CT

In recent years, dual-energy imaging technology has evolved outstandingly, enabling to perform first pass myocardial CTP with promising results, improving limitations that are commonly present in SECT such as BHA and blooming artifacts (BA).

DECT allows a functional evaluation based on tissue analysis according to the chemical composition. In this way, tissue alterations can be observed even in cases with no morphological findings.

The basic requirements to carry out a dual energy/spectral CT are the following:
(I)   X rays sources providing X rays quanta with different energies;
(II)   Detector technology able to differentiate diverse quanta at dissimilar energies;
(III) Tissues with sufficient difference between material densities on diverse energies.

Tissue attenuations measured by CT is characterized by three physical processes:
(I)   Compton scatter, which is the largest component of attenuation in relation to electron density;
(II)   Rayleigh scatter, related to the electrons (only constitutes a minimum amount);
(III) Photoelectric effect, closely related the atomic z number of the material (number of protons of the atomic core).

DECT permits better analysis of tissues that have significant differences in Z values at different spectral range. The elements that work best with DECT are those with high atomic number such as iodine (z=53) and calcium (z=20), having different behavior between low and high energy levels. In the other hand, elements with low atomic number such as hydrogen (z=1), oxygen (z=8), carbon (z=6) or nitrogen (z=7) have no important differences across the energy levels.

DECT approaches

DECT acquisition can be classified into two groups: source oriented and detector oriented.

Source oriented (Siemens Healthcare)

This approach relies on the X-ray source to generate X-rays with two different energy spectra by scanning from 2 different X-ray tubes. The two tubes are placed within the same rotation gantry with an angular offset of 90° (first generation) or 94° (second generation), where one tube operates at 80 kVp and the second one at 140 kVp. Only one detector can cover a field of view of 50 cm and the second one can cover 26 or 33 cm according to the gantry generation.

A potential problem is related to increased scatter radiation from 2 tubes that can lead to shaded artifacts in reconstructed images. Also, material decomposition (MD) can be affected as well as BHA correction can be suboptimal on monochromatic images.

Detector oriented

In this approach there are two options: kV power switching or dual layer detector technology.

kVp switching (GE Healthcare)

In this option only one tube works in an ultrafast switching (0.2 ms) between low and high tube potentials. The detector has the ability to discriminate between low and high energy X-ray photons in a single X-ray beam. Each pair of 80 and 140 kV projections are obtained with similar view angle. In order to avoid spectral contamination, the scanner has a scintillating material known as Gemstone that has an ultrafast primary decay time (0.03 microseconds) and low afterglow (delayed fluorescence). Due to the minimal view angle mismatch between low and high tube potentials projections, MD can be performed in the projection space more accurately. The main disadvantage of this approach is related to the inability to modulate the tube-current with tube potential giving image sets at different noise levels. Although iterative reconstruction can be applied, lower energy levels are nosier in relation to higher levels.

Dual layer detector (Philips Medical Systems)

In this system, the X-ray detector comprises two different scintillating materials attached together. The upper layer is 1 mm thick, composed by Zinc Selenide (ZnSe) and the bottom layer is 2 mm thick, composed by Gadolinium orthosilicate (GOS). This technologic approach permits higher energy X-ray photons to pass through the upper level without suffering significant interaction, whereas the lower energy photons are mostly diminished in the top layer. The two signals would look like two X-rays in 2 different energy ranges.

The principal advantage of this strategy is that at each view the high- and low-energy projections are exactly obtained with respect to each other. Nonetheless, a potential problem is there is less spectral separation between both energy projections that can lead to an inaccurate MD and BHA correction.

Data acquisition protocols using DECT

Scanning techniques

Similar to single energy myocardial CTP, DECT also requires in most cases two CT scans in stress and rest. The type of scanning CT technique will vary according to the CT system (63,64).

Scanning with dual source CT scanner

For the stress scan, DECT studies with dual source CT scanners are acquired with retrospective ECG-gating mode and tube current modulation, to obtain systolic as well as diastolic phases. Technical parameters vary according to the scanner generation.

First generation: Gantry rotation time: 330-ms, detectors: 32×2, pitch: 0.2 to 0.43 (according to the heart rate), slice thickness: 1.5 mm (stress); 0.6 mm (rest), tube current and voltage: tube A, 150 mA/rotation at 140 kV; tube B, 165 mA/rotation at 80 kV.

Second generation: Gantry rotation time: 280-ms, pitch: 0.17 to 0.2 (according to the heart rate) detectors: 2×64, slice thickness: 1.5 mm (stress); 0.6 mm (rest), tube current and voltage: tube A, 140 mA/rotation at 140 kV; tube B, 165 mA/rotation at 80 kV.

For patients with high and/or irregular heart rate a wider window is required (i.e., 37–75%) whereas for others with low and regular heart rates a narrow window is enough (i.e., 60–70%). For the rest scan if heart rate needed returns to baseline, only mid-diastolic phase (75%) with no padding is used.

### Scanning with single source CT scanner with kVp switching

For cardiac imaging, these DECT scanners only acquire in a prospective ECG-gated mode, and both stress-rest scans have to be performed in an axial mode. Both acquisitions have similar parameters differing only in the extent of padding required for the acquisition and the centered phase. For the stress scan a wider padding needs to be selected as systolic and diastolic phases are needed.

After the vasodilator, the majority of the patients experience a mild increase in heart rate. According to the increment in heart rate, center phase and padding have to be adjusted. If heart rate raises to >75 bpm, a center phase at 60% with 150 ms padding are selected, whereas if the heart rate is around 65 bpm or lower, the padding should be increased to 200–250 ms.

For the rest scan, a CT scan with center phase at 75% phase is performed. A complementary padding (82–100 ms) can be added according to the heart rate.

Scanning with dual layer

Stress scan can be performed in retrospective ECG-gated mode with tube current modulation and rest scan in
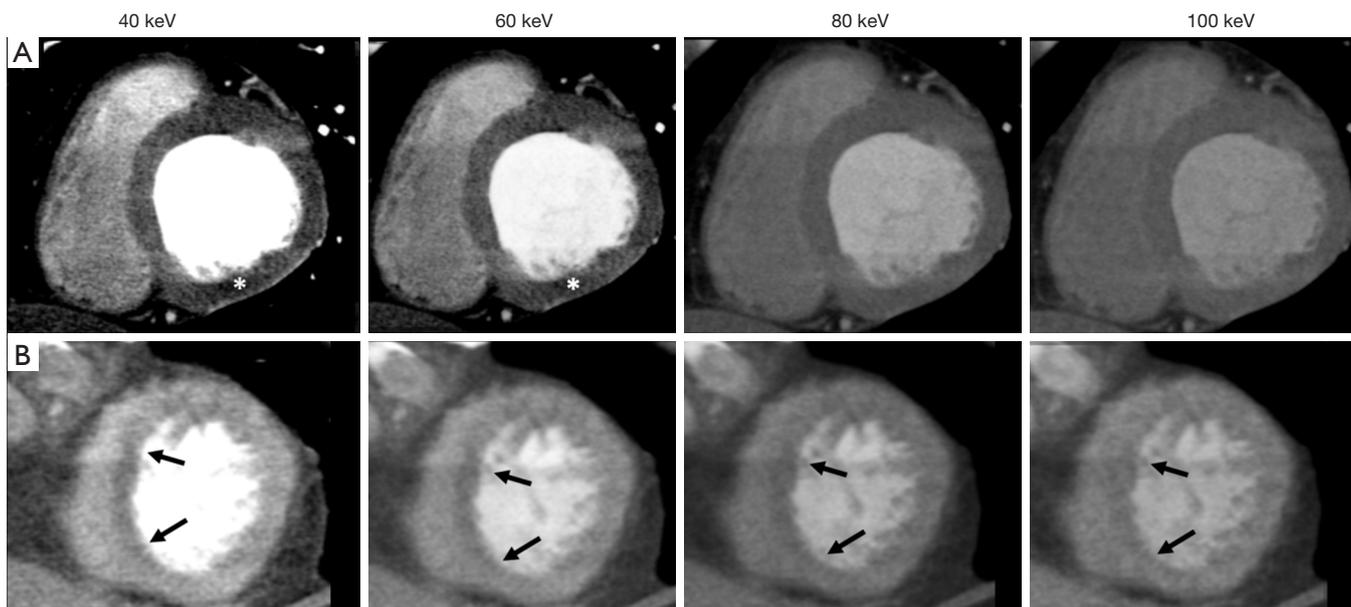
Figure 3 Beam hardening artifact versus true perfusion defects. (A) Short axis at 40, 60, 80 and 100 keV showing a myocardial perfusion defect in the inferobasal wall (segment 5) present at 40 and 60 keV (asterisk). At 80 keV the defect disappears demonstrating that correspond to a Beam Hardening Artifact; (B) short axis at 40, 60, 80 and 100 keV showing a septal hypoperfusion that persists at all energy levels confirming the presence of a true perfusion defect.

prospective ECG-gated mode to reduce radiation dose.

DECT post-processing and analysis

DECT imaging enables different types of image analysis that can significantly reduce BHA and BA.

Polychromatic images

Also known as mixed images, mimic SECT images (64). They are obtained by linear weighting of the CT attenuation value for the two spectra and correspond to an intermediate energy level.

Monochromatic examination

Virtual monochromatic images (VMI) (65) are obtained applying attenuation measurements in two basic materials such as iodine and water, which are transformed into densities obtained from low and high voltage peak projections and then rebuilt to originate the base material image pairs. Monochromatic examination allows the visualization of the tissues at different energy levels ranging from 40 to 140 keV (Siemens and GE) and up to 200 keV

(Philips). Low energy levels show higher intraluminal and tissue enhancement, allowing reducing the amount of contrast load required. Image noise has to be reduced applying iterative reconstruction. Mid energy levels ranging from 77 to 100 keV are the best to reduce or even cancel BHA and BA.

As aforementioned, BHA typically appear in sites where two adjacent structures with high density suffer from material inhomogeneity, and can cause false myocardial perfusion defects in certain myocardial segments such as posterobasal (AHA segment 5) and apical segments.

At low energy levels around 40 keV, both BHA and true perfusion defects look similar. However, perfusion defects caused by BHA start to attenuate as monoenergetic levels increase, and commonly disappear at levels above 80 to 100 keV. On the contrary, a true perfusion defect should persist at all energy levels (*Figure 3*). Both grayscale and color scale can be utilized for analysis, and ischemic defects are better identified at low energy levels (40 keV) (*Figure 4*).

BA can also be reduced using monochromatic analysis at medium energy levels. BA overestimates the size of calcified plaques, leading to inaccurate stenosis measurements. In cases of severe calcification, DECT could improve stenosis quantification in this selected group of patients leading to
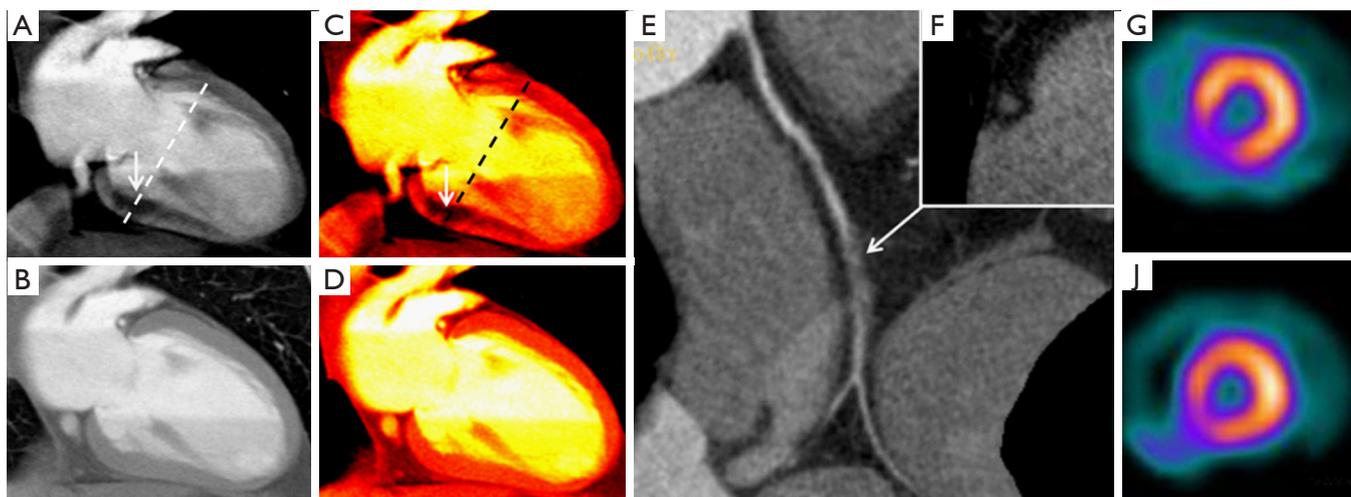
Figure 4 Stress-rest dual energy CT myocardial perfusion. A 48-year-old female, with typical chest pain. Body mass index 27 kg/m^2. Cardiovascular risk factors: hypertension, hypercholesterolemia, smoking. Functional tests demonstrate mild infero-septal ischemia. (A) Stress dual energy CT (40 keV) at long axis demonstrates a severe hypo-perfusion at inferior basal wall (arrow); (B) rest dual energy imaging shows normal (homogeneous) myocardial perfusion; (C,D) same DECT images using color-coding to highlight the perfusion deficit; (E) curved multiplanar reconstruction of the right coronary artery showing a critical sub-occlusive stenosis due to a non-calcified plaque (arrow); (F) orthogonal view in the area of the stenosis; (G) stress SPECT short axis showing severe infero-septal defect (arrow); (H) rest SPECT short axis: almost complete perfusion recovery.

an increased accuracy of CAD.

MD

It is based upon different attenuation coefficients of various tissues, which in turn depend on the energy levels of the X-ray beam (66). MD harvests knowledge about tissue atomic number and can deliver "mass density maps", for basic materials such as water or iodine. They can give information of the concentration of a given material (mg/Ugr/mm^3) in the myocardium. In myocardial perfusion imaging, the amount of iodine can be measured in order to establish normal or an abnormal perfusion.

Clinical evidence in DECT

As above mentioned, myocardial CTP can be accurately assessed using single energy (SECT) acquisitions. Nonetheless, the presence of BHA related to the polychromatic nature of X-rays often leads to the areas of myocardial hypoattenuation that can mimic hypoperfusion specific left ventricular segments. Instead, DECT has emerged as a potential means to attenuate or even cancel such artifacts.

A number of clinical studies have explored the role of DECT for the assessment of CTP (*Table 2*).

Arnoldi *et al.* were among the first to evaluate the diagnostic performance of DECT versus SECT for the detection of myocardial blood volume deficit, using SPECT as reference standard (72). Using a dual source scanner, DECT raw data was analyzed using: (I) high energy (140 kV), (II) low energy (80 or 100 kV), (III) mixed (30% low/70% high), and (IV) iodine maps. In this study, the assessment using iodine maps achieved the highest sensitivity, negative predictive value, and accuracy of 91%, 97% and 93% for the detection of mixed and fixed perfusion defects.

The diagnostic performance of adenosine-stress first-pass dual-energy CTP was also compared to adenosine-stress dynamic real-time CTP for the assessment of patients with acute chest pain (73). In this study, Weininger *et al.* reported that 80% of myocardial segments were assessable in the dynamic CTP perfusion group, with a sensitivity of 86% and a specificity of 98% compared to CMR, and 84% and 92%, compared to SPECT, respectively. In turn, all segments were assessable within the static CTP group, with a sensitivity of 93% and specificity of 99% (*vs.* CMR), and of 94% and 98% (*vs.* SPECT).

Table 2 Studies assessing myocardial CT perfusion using dual energy CT

Study	Number of Patients	Reference standard		Sensitivity (%, per segment)	Specificity (%, per segment)	Radiation dose
Meinel *et al.* (67)	55	SPECT		99.0	97.0	Rest: 5.6 mSv; stress: 7.1 mSv; LE: 4.7 mSv
Ko *et al.* (68)	45	Invasive Angiography	CTA	91.8	67.7	Stress: 10.8±2.5 mSv
			CTA + CTP	93.2	85.5	Rest: 5.7±0.5 mSv
Kido *et al.* (69)	25	Invasive Angiography	CTA	83.3	74.4	Stress-Rest: 7.7±2.8 mSv
			CTA + CTP	66.7	92.3	–
De Cecco *et al.* (70)	29	SPECT Invasive Angiography	CTA	95.0	50.0	Rest: 5.8 mSv
			CTP	95.0	50.0	Stress: 6.6 mSv
			CTA + CTP	90.0	67.0	LE: 4.5 mSv
Carrascosa *et al.* (71)	25	SPECT	CTA	66.7	72.4	Rest: 3.2±0.4 mSv
			CTP	73.7	94.7	Stress: 4.3±1.1 mSv
			CTA + CTP	56.0	97.0	Total: 7.5±1.2 mSv

More recently, Meinel *et al.* explored the accuracy of DECT using a dual-source CT scanner for the assessment of myocardial blood supply among 55 patients with known or suspected CAD and indication of SPECT (67). The sensitivity and specificity for the detection of any perfusion defect was 92% and 98% for the rest-only evaluation; whereas for the stress-only, rest/stress, stress plus delayed enhancement, and stress/rest plus delayed enhancement was 99% and 97%, respectively. Of note, 13 of the 29 (45%) segments showing reversible perfusion defects at SPECT were misclassified by rest-stress DECT as fixed perfusion defects.

The effect of BHA reduction for the assessment of myocardial CTP was further assessed by Carrascosa *et al.* (74) In this prospective study including patients with intermediate to high likelihood of CAD, the authors demonstrated that DECT had a significantly higher diagnostic performance than SECT for the detection of perfusion defects [AUC 0.90 (95% CI, 0.86–0.94) *vs.* 0.80 (95% CI, 0.76–0.84), P=0.0004]. Notably, similar results were obtained when including only segments affected by BHA [AUC 0.90 (95% CI, 0.84–0.96) *vs.* 0.77 (95% CI, 0.69–0.84), P=0.007].

More recently, the same group specifically reported the role of DECT dual energy for the reduction of BHA in myocardial perfusion studies (59). For this purpose, the authors included patients referred for a CTA with normal SPECT and absence or only mild coronary atherosclerosis. The control group was acquired using SECT. Significant

signal density differences were identified between the posterobasal segment (the segment most commonly affected by BHA) and the reference segment among the lower energy levels, whereas such differences were attenuated and/or cancelled at ≥70 keV, achieving homogeneous signal density levels.

A recent study has explored the optimal energy levels for the assessment of CTP. The authors reported a sensitivity, specificity, positive predictive value, and negative predictive value of DE-CTP for the detection of perfusion defects of 84%, 94%, 77%, and 96%; respectively. Furthermore, the authors found that the largest differences in signal density between segments with normal perfusion and those with perfusion defects were identified among low energy levels, with a sensitivity of 96% and specificity of 98% using a cut-off value ≤153 HU at 40 keV, progressively declining at higher levels (75).

Combined evaluation CCTA and CTP

Wang *et al.* were among the first to evaluate the incremental value of CTP using DECT over CCTA among 34 patients with known CAD or abnormal SPECT (76). In this study, the combined assessment of CTP plus CCTA (with a sensitivity of 82% and specificity of 91%) achieved improved diagnostic performance compared to the individual use of CCTA or CTP with DECT.

Similarly, Kido *et al.* explored the incremental value of the combined CCTA plus adenosine stress-CTP among

patients undergoing ICA (69). In this study, myocardial CTP derived from DECT was assessed using color-coded iodine maps. Of note, 62% of the patients could be evaluated by CCTA alone (due to severe calcification or motion) compared to 100% with CTP, with a diagnostic accuracy of 83% of the combined assessment, compared to 78% with the CTA alone.

Ko *et al.* (68) studied 45 patients with suspected CAD using ICA as the reference standard method. Authors evaluated the potential incremental value that DE-CTP could provide to CCTA. Each patient presented at least one severe lesion by ICA. Results of CCTA alone included a sensitivity of 92% and a specificity of 67%, whereas CCTA plus DE-CTP showed a sensitivity of 93% and a specificity of 86%. Authors concluded that DECT may reduce false positive results.

In a small study including a high-risk population for CAD, De Cecco *et al.* reported a reduced number of false-positives with the combined assessment (70).

Finally, using a single source DECT scanner with kVp switching among 25 patients with intermediate to high likelihood of CAD, Carrascosa *et al.* demonstrated that stress myocardial perfusion added a significant incremental value over CTA alone [AUC 0.84 (95% CI, 0.80–0.87) *vs.* 0.70 (95% CI, 0.65–0.74), P=0.003] (71).

Image analysis

Results may be displayed using color-coded maps, where the shading represents particular myocardial perfusion values, such as myocardial blood flow or volume. The voxel-based functional imaging maps may be sampled for (averaged) regional perfusion values. While semi-quantification of myocardial perfusion values should be used to differentiate normal, ischemic, and infarcted myocardium, there is no accepted positive criterion with threshold values that may be applied for interpretation. Thus, currently, relative differences in perfusion values between different myocardial segments have been adopted in clinical scenarios.

It is necessary to perform a combined anatomic and perfusion interpretation. Rest CT scan is mainly used to determine the presence or absence of CAD. In the case of coronary stenosis, determination of the grade of the stenosis orients in the evaluation of a possible myocardial perfusion defect. For this analysis, a combination of axial, multiplanar reformats (MPR), maximum intensity projections (MIP), curved multiplanar reformats (cMPR) and volume rendering technique (VRT) reconstructions can be used (77).

Myocardial analysis consists in the evaluation of the myocardium in short axis views from the apex to the base of the left ventricle, using the 17 segments suggested by the AHA classification. In general segment 17 (apical segment) is better assessed in a long axis view or four chamber view.

It is important to pay attention for possible artifacts that can appear especially in SECT in certain myocardial segments that can mimic myocardial perfusion defects. For that reason it is important to correlate anatomic with perfusion findings.

DECT can better assess myocardial perfusion as applying monochromatic evaluation at different energy levels in the same axis than SECT can confirm or rule out a true perfusion.

Myocardial hypoattenuated areas present at low energy levels (40 keV) that tend to or disappear at medium to high levels (77–100 keV) correspond to a BHA, whereas if the defect persists at all energy levels it constitutes a true myocardial perfusion defect.

Also, DECT can apply MD and create iodine maps being able to measure the amount of iodine in the myocardial wall.

Myocardial perfusion defects in rest can only be attributed to ischemia in acute scenarios when a vessel is abruptly occluded or in severe stenosis larger than 90% (rest ischemia).

Stress-CTP scans are used exclusively to identify or rule out perfusion defects. In general, as patients experience mild increments in the heart rate after vasodilation, is necessary to analyze both systolic and diastolic phases. Higher heart rates are associated with more suitable temporal resolution in systolic phases, although images in this phase are particularly prone to heart-rate related artifacts. Accordingly, the reading physician should be trained in the recognition of artifacts that can lead to inaccurate diagnosis.

For stress CTP interpretation, images of the myocardium are typically examined with short, vertical, and horizontal axis, using a narrow window width and level settings (W200-300/L100-150) and an average slice thickness of 3 to 5 mm. Any perfusion defect should be confirmed in at least two views (78,79).

In the case where a true perfusion defect is diagnosed in stress, the physician should evaluate at the rest scan the corresponding coronary artery that supplies the underlying myocardium in order to confirm if there is a moderate or severe stenosis causing such perfusion defect. The behavior of the perfusion defect in stress and rest will also allow to establish if it corresponds to myocardial ischemia (it will

normalize at rest).

CTP analysis should be performed using a qualitative data analysis, but can also be complemented using semi-quantitative data by measuring Hounsfield units and calculating the TPR. TPR is the ratio of the sector specific subendocardial attenuation and the mean subepicardial attenuation of the entire subepicardial layer of any given short axis slice. The TPR is considered abnormal when it was <0.99 (37).

Standard cardiac planes in short-axis, horizontal and vertical long axis views with a narrow window and level have to be used in average or minimum intensity projection modes. MIP should not be used as they can mask perfusion defects. To facilitate detection of myocardial perfusion defects it is useful to compare short axis views in stress and rest. Suspicious or doubtful artifacts appearing like myocardial perfusion defects have to be reported.

Conclusions

It is mandatory not only to detect the presence of CAD but also to evaluate in cases of moderate or moderate to severe stenosis the functional relevance that the stenosis is generating in order to establish the best therapeutic decision for the patient.

CCTA alone has a very high negative predictive value to exclude CAD, although it has a relatively poor positive predictive value to determine the presence of ischemia. Rest perfusion defects can only be detected by CCTA in cases of severe stenosis >90% or in acute scenarios with total vessel occlusion. For that reason, a stress study might be required to determine the presence and amount of ischemia. Although there are many modalities that can be used to associate to the anatomical evaluation such as SPECT, CMR, stress echo, and PET, none of them allow a comprehensive anatomo-functional evaluation within a single session. CTP, in combination with CCTA, has emerged as a good option to study these patients. Several clinical investigation including multicenter studies performed both using SECT and DECT have demonstrated that myocardial CTP has good results, with total radiation doses that are currently lower than 9 mSv, thereby potentially enabling the clinical application of this technique among selected patients as an alternative for the aforementioned diagnostic tools.

Acknowledgements

None.

Footnote

References

1. McCollough CH, Zink FE. Performance evaluation of a multi-slice CT system. Med Phys 1999;26:2223-30.
2. Rydberg J, Buckwalter KA, Caldemeyer KS, et al. Multisection CT: scanning techniques and clinical applications. Radiographics 2000;20:1787-806.
3. Kelly DM, Hasegawa I, Borders R, et al. High-resolution CT using MDCT: comparison of degree of motion artifact between volumetric and axial methods. AJR Am J Roentgenol 2004;182:757-9.
4. Douglas PS, Hoffmann U, Patel MR, et al. PROMISE Investigators. Outcomes of anatomical versus functional testing for coronary artery disease. N Engl J Med 2015;372:1291e1300.
5. SCOT-HEART investigators. CT coronary angiography in patients with suspected angina due to coronary heart disease (SCOT-HEART): an open-label, parallel-group, multicentre trial. Lancet 2015;385:2383-91.
6. Goldstein JA, Chinnaiyan KM, Abidov A, et al. The CT-STAT (Coronary Computed Tomographic Angiography for Systematic Triage of Acute Chest Pain Patients to Treatment) trial. J Am Coll Cardiol 2011;58:1414e1422.
7. Litt HI, Gatsonis C, Snyder B, et al. CT angiography for safe discharge of patients with possible acute coronary syndromes. N Engl J Med. 2012;366:1393e1403.
8. Hoffmann U, Truong QA, Schoenfeld DA, et al. Coronary CT angiography versus standard evaluation in acute chest pain. N Engl J Med. 2012;367:299e308.
9. Hamilton-Craig C, Fifoot A, Hansen M, et al. Diagnostic performance and cost of CT angiography versus stress ECGea randomized prospective study of suspected acute coronary syndrome chest pain in the emergency department (CT- COMPARE). Int J Cardiol 2014;177:867e873.
10. Cury RC, Feuchtner G, Battle J, et al. Triage of patients presenting with chest pain to the emergency department: implementation of coronary CTA in a large urban hospital healthcare system. Am J Roentgenol 2013;200:57e65.
11. Poon M, Cortegiano M, Abramowicz AJ, et al. Associations between routine coronary computed tomographic angiography and reduced unnecessary hospital admissions,

length of stay, recidivism rates, and invasive coronary angiography in the emergency department triage of chest pain. J Am Coll Cardiol 2013;62:543e552.

12. Miller JM, Rochitte CE, Dewey M, et al. Diagnostic performance of coronary angiography by 64-row CT. N Engl J Med 2008;359:2324-36.

13. Budoff MJ, Dowe D, Jollis JG, et al. Diagnostic performance of 64-multidetector row coronary computed tomographic angiography for evaluation of coronary artery stenosis in individuals without known coronary artery disease: results from the prospective multicenter ACCURACY (Assessment by Coronary Computed Tomographic Angiography of Individuals Undergoing Invasive Coronary Angiography) trial. J Am Coll Cardiol 2008;52:1724-32.

14. Meijboom WB, Meijs MF, Schuijf JD, et al. Diagnostic accuracy of 64-slice computed tomography coronary angiography: a prospective, multicenter, multivendor study. J Am Coll Cardiol 2008;52:2135-44.

15. Sun J, Zhang Z, Lu B, et al. Identification and quantification of coronary atherosclerotic plaques: a comparison of 64-MDCT and intravascular ultrasound. AJR Am J Roentgenol 2008;190:748-54.

16. Carrascosa PM, Capuñay CM, Garcia-Merletti P, et al. Characterization of coronary atherosclerotic plaques by multidetector computed tomography. Am J Cardiol 2006;97:598-602.

17. Leber AW, Knez A, von Ziegler F, et al. Quantification of obstructive and nonobstructive coronary lesions by 64-slice computed tomography: a comparative study with quantitative coronary angiography and intravascular ultrasound. J Am Coll Cardiol 2005;46:147-54.

18. Cury RC, Abbara S, Achenbach S, et al. CAD-RADS(TM) Coronary Artery Disease - Reporting and Data System. An expert consensus document of the Society of Cardiovascular Computed Tomography (SCCT), the American College of Radiology (ACR) and the North American Society for Cardiovascular Imaging (NASCI). Endorsed by the American College of Cardiology. J Cardiovasc Comput Tomogr 2016;10:269-81.

19. Strauss HW, Harrison K, Langan JK, et al. Thallium-201 for myocardial imaging. Relation of thallium-201 to regional myocardial perfusion. Circulation 1975;51:641-5.

20. Berman DS, Kiat HS, Van Train KF, et al. Myocardial perfusion imaging with technetium-99m-sestamibi: comparative analysis foravailable imaging protocols. J Nucl Med 1994;35:681-8.

21. Hung GU, Lee KW, Chen CP, et al. Relationship of transient ischemic dilation in dipyridamole myocardial perfusion imaging and stress-induced changes of functional parameters evaluated by Tl-201 gated SPECT. J Nucl Cardiol 2005;12:268-75.

22. Abidov A, Bax JJ, Hayes SW, et al. Transient ischemic dilation ratio of the left ventricle is a significant predictor of future cardiac events in patients with otherwise normal myocardial perfusion SPECT. J Am Coll Cardiol 2003;42:1818-25.

23. Greenwood JP, Maredia N, Younger JF, et al. Cardiovascular magnetic resonance and single-photon emission computed tomography for diagnosis of coronary heart disease (CE-MARC). A prospective trial. Lancet 2012;379:453-60.

24. Hundley WG, Hamilton CA, Thomas MS, et al. Utility of fast cine magnetic resonance imaging and display for the detection of myocardial ischemia in patients not well suited for second harmonic stress echocardiography. Circulation 1999;100:1697-702.

25. Al-Saadi N, Nagel E, Gross M, et al. Noninvasive detection of myocardial ischemia from perfusion reserve based on cardiovascular magnetic resonance. Circulation 2000;101:1379-83.

26. Manning WJ, Atkinson DJ, Grossman W, et al. First-pass nuclear magnetic resonance imaging studies using gadolinium-DTPA in patients with coronary artery disease. J Am Coll Cardiol 1991;18:959-65.

27. Wilke N, Jerosch-Herold M, Wang Y, et al. Myocardial perfusion reserve: assessment with multisection, quantitative, first-pass MR imaging. Radiology 1997;204:373-84.

28. Heijenbrok-Kal MH, Fleischmann KE, Hunink MG. Stress echocardiography, stress singlephoton- emission computed tomography and electron beam computed tomography for the assessment of coronary artery disease: a meta-analysis of diagnostic performance. Am Heart J 2007;154:415-23.

29. Dawson D, Rinkevich D, Belcik T, et al. Measurement of myocardial blood flow velocity reserve with myocardial contrast echocardiography in patients with suspected coronary artery disease: comparison with quantitative gated Technetium 99m sestamibi single photon emission computed tomography. J Am Soc Echocardiogr 2003;16:1171-7.

30. Armstrong WF, Zoghbi WA. Stress echocardiography: current methodology and clinical applications. J Am Coll Cardiol 2005;45:1739-47.

31. Dorbala S, Hachamovitch R, Curillova Z, et al.

Incremental prognostic value of gated Rb-82 positron emission tomography myocardial perfusion imaging over clinical variables and rest LVEF. JACC Cardiovasc Imaging 2009;2:846-54.

32. Gould RG, Lipton MJ, McNamara MT, et al. Measurement of regional myocardial blood flow in dogs by ultrafast CT. Invest Radiol 1988;23:348-53.

33. Garcia MJ, Lessick J, Hoffmann MH. Accuracy of 16-row multidetector computed tomography for the assessment of coronary artery stenosis. JAMA 2006;296:403-11.

34. Kurata A, Mochizuki T, Koyama Y, et al. Myocardial perfusion imaging using adenosine triphosphate stress multi-slice spiral computed tomography: alternative to stress myocardial perfusion scintigraphy. Circ J 2005;69:550-7.

35. George RT, Silva C, Cordeiro MA, et al. Multidetector computed tomography myocardial perfusion imaging during adenosine stress. J Am Coll Cardiol 2006;48:153-60.

36. Blankstein R, Shturman LD, Rogers IS, et al. Adenosine-induced stress myocardial perfusion imaging using dual-source cardiac computed tomography. J Am Coll Cardiol 2009;54:1072-84.

37. George RT, Arbab-Zadeh A, Miller JM, et al. Adenosine stress 64- and 256-row detector computed tomography angiography and perfusion imaging: a pilot study evaluating the transmural extent of perfusion abnormalities to predict atherosclerosis causing myocardial ischemia. Circ Cardiovasc Imaging 2009;2:174-82.

38. Tamarappoo BK, Gutstein A, Cheng VY, et al. Assessment of the relationship between stenosis severity and distribution of coronary artery stenoses on multislice computed tomographic angiography and myocardial ischemia detected by single photon emission computed tomography. J Nucl Cardiol 2010;17:791-802.

39. Feuchtner G, Goetti R, Plass A, et al. Adenosine stress high-pitch 128-slice dual-source myocardial computed tomography perfusion for imaging of reversible myocardial ischemia: comparison with magnetic resonance imaging. Circ Cardiovasc Imaging 2011;4:540-9.

40. George RT, Arbab-Zadeh A, Miller JM, et al. Computed tomography myocardial perfusion imaging with 320-row detector computed tomography accurately detects myocardial ischemia in patients with obstructive coronary artery disease. Circ Cardiovasc Imaging 2012;5:333-40.

41. Ko BS, Cameron JD, Meredith IT, et al. Computed tomography stress myocardial perfusion imaging in patients considered for revascularization: a comparison with fractional flow reserve. Eur Heart J 2012;33:67-77.

42. Ko BS, Cameron JD, Leung M, et al. Combined CT coronary angiography and stress myocardial perfusion imaging for hemodynamically significant stenoses in patients with suspected coronary artery disease: a comparison with fractional flow reserve. JACC Cardiovasc Imaging 2012;5:1097-111.

43. Bettencourt N, Chiribiri A, Schuster A, et al. Direct comparison of cardiac magnetic resonance and multidetector computed tomography stress-rest perfusion imaging for detection of coronary artery disease. J Am Coll Cardiol 2013;61:1099-107.

44. Kikuchi Y, Oyama-Manabe N, Naya M, et al. Quantification of myocardial blood flow using dynamic 320-row multi-detector CT as compared with (1)(5) O-H(2)O PET. Eur Radiol 2014;24:1547-56.

45. Cury RC, Kitt TM, Feaheny K, et al. A randomized, multicenter, multivendor study of myocardial perfusion imaging with regadenoson CT perfusion vs single photon emission CT. J Cardiovasc Comput Tomogr 2015;9:103-12.e1-2.

46. George RT, Mehra VC, Chen MY, et al. Myocardial CT Perfusion Imaging and SPECT for the Diagnosis of Coronary Artery Disease: A Head-to-Head Comparison from the CORE320 Multicenter Diagnostic Performance Study. Radiology 2015;274:626.

47. Uren NG, Melin JA, De Bruyne B, et al. Relation between myocardial blood flow and the severity of coronary-artery stenosis. N Engl J Med 1994;330:1782-8.

48. Kim HL, Kim YJ, Lee SP, et al. Incremental prognostic value of sequential imaging of single-photon emission computed tomography and coronary computed tomography angiography in patients with suspected coronary artery disease. Eur Heart J Cardiovasc Imaging 2014;15:878-85.

49. Caballeros M, Bartolomé P, Fernández González Ó, et al. Effect of contrast dose in the quantification of myocardial extra-cellular volume in adenosinestress/rest perfusion cardiac magnetic resonance examinations. Acta Radiol 2016. [Epub ahead of print].

50. Bodi V, Sanchis J, Lopez-Lereu MP, et al. Prognostic and therapeutic implications of dipyridamole stress cardiovascular magnetic resonance on the basis of the ischaemic cascade. Heart 2009;95:49-55.

51. Ghimire G, Hage FG, Heo J, et al. Regadenoson: a focused update. J Nucl Cardiol 2013;20:284-8.

52. Kwon DH, Cerqueira MD, Young R, et al. Lessons from regadenoson and low-level treadmill/regadenoson myocardial perfusion imaging: initial clin- ical experience

in 1263 patients. J Nucl Cardiol 2010;17:853-7.

53. Golzar Y, Doukky R. Regadenoson use in patients with chronic obstructive pulmonary disease: the state of current knowledge. Int J Chron Obstruct Pulmon Dis 2014;9:129-37.

54. Lin LF, Cheng CY, Hou CH, et al. Experience of low-dose aminophylline use to relieve minor adverse effects of dipyridamole in patients undergoing stress myocardial perfusion imaging. J Nucl Cardiol 2014;21:563-9.

55. Johnson NP, Lance Gould K. Dipyridamole reversal using theophylline during aminophylline shortage. J Nucl Cardiol 2011;18:1115.

56. Rochitte CE, George RT, Chen MY, et al. Computed tomography angiography and perfusion to assess coronary artery stenosis causing perfusion defects by single photon emission computed tomography: the CORE320 study. Eur Heart J 2014;35:1120-30.

57. Takx RA, Suchá D, Park J, et al. Sublingual Nitroglycerin Administration in Coronary Computed Tomography Angiography: a Systematic Review. Eur Radiol 2015;25:3536-42.

58. Deseive S, Chen MY, Korosoglou G, et al. Prospective Randomized Trial on Radiation Dose Estimates of CT Angiography Applying Iterative Image Reconstruction: The PROTECTION V Study. JACC Cardiovasc Imaging 2015;8:888-96.

59. Carrascosa P, Rodriguez-Granillo GA, Capuñay C, et al. Low-dose CT coronary angiography using iterative reconstruction with a 256-slice CT scanner. World J Cardiol 2013;5:382-6.

60. Rodriguez-Granillo GA, Carrascosa P, Cipriano S, et al. Beam hardening reduction using dual energy computed tomography: implications for myocardial perfusion studies. Cardiovasc Diagn Ther 2015;5:79-85.

61. Rocha-Filho JA, Blankstein R, Shturman L, et al. Incremental value of adenosine-induced stress myocardial perfusion imaging with dual-source CT at cardiac CT angiography. Radiology 2010;254:410-9.

62. Rief M, Zimmermann E, Stenzel F, et al. Computed tomography angiography and myocardial computed tomography perfusion in patients with coronary stents: prospective intraindividual comparison with conventional coronary angiography. J Am Coll Cardiol 2013;62:1476-85.

63. Schwarz F, Ruzsics B, Schoepf UJ, et al. Dual-energy CT of the heart--principles and protocols. Eur J Radiol 2008;68:423-33.

64. Yu L, Primak AN, Liu X, et al. Image quality optimization and evaluation of linearly mixed images in dual-source,

dual-energy CT. Med Phys 2009;36:1019-24.

65. Matsumoto K, Jinzaki M, Tanami Y, et al. Virtual monochromatic spectral imaging with fast kilovoltage switching: improved image quality as compared with that obtained with conventional 120-kVp CT. Radiology 2011;259:257-62.

66. Johnson TR, Krauss B, Sedlmair M, et al. Material differentiation by dual energy CT: initial experience. Eur Radiol 2007;17:1510-7.

67. Meinel FG, Cecco C, Schoepf UJ, et al. First–arterial-pass dual-energy CT for assessment of myocardial blood supply: do we need rest, stress, and delayed acquisition? Comparison with SPECT. Radiology 2014;270:708-16.

68. Ko SM, Choi JW, Hwang HK, et al. Diagnostic performance of combined noninvasive anatomic and functional assessment with dual source CT and adenosine induced stress dual energy CT for detection of significant coronary stenosis. AJR Am J Roentgenol 2012;198:512-20.

69. Kido T, Watanabe K, Saeki H. Adenosine triphosphate stress dual source computed tomography to identify myocardial ischemia: comparison with invasive coronary angiography. Springer Plus 2014;3:75.

70. De Cecco CN, Harris B, Schoepf U, et al. Incremental value of pharmacological stress cardiac dual-energy CT over coronary CT angiography alone for the assessment of coronary artery disease in a high-risk population. AJR Am J Roentgenol 2014;203:W70-7.

71. Carrascosa PM, Deviggiano A, Capuñay C, et al. Incremental value of myocardial perfusion over coronary angiography by spectral computed tomography in patients with intermediate to high likelihood of coronary artery disease. Eur J Radiol 2015;84:637-42.

72. Arnoldi E, Lee YS, Ruzsics B, et al. Ct detection of myocardial blood volumen deficits: dual-energy CT compared with single energy Ct spectra. J Cardiovasc Comput Tomogr 2011;5:421-9.

73. Weininger M, Schoepf UJ, Ramachandra A, et al. Adenosine-stress dynamic real-time myocardial perfusion and adenosine-stress first-pass dual-energy myocardial perfusion CT for the assessment of acute chest pain: initial results. Eur J Radiol 2012;81:3703-10.

74. Carrascosa PM, Cury R, Deviggiano A, et al. Myocardial perfusion evaluation with single versus dual energy CT: impact of beam hardening artifacts. Acad Radiol 2015;22:591-9.

75. Carrascosa P, Deviggiano A, de Zan M, et al. Improved discrimination of myocardial perfusion defects at low energy levels using virtual monochromatic imaging. J

Comput Assist Tomogr 2017. [Epub ahead of print].

76. Wang R, Yu W, Wang Y, et al. Incremental value of dual-energy CT to coronary CT angiography for the detection of significant coronary stenosis: comparison with quantitative coronary angiography and single photon emission computed tomography. Int J Cardiovasc Imaging 2011;27:647-56

77. Cademartiri F, Mollet N, Lemos PA, et al. Standard versus user-interactive assessment of significant coronary stenoses with multislice computed tomography coronary

angiography. Am J Cardiol 2004;94:1590-3.

78. Leipsic J, Abbara S, Achenbach S, et al. SCCT guidelines for the interpretation and reporting of coronary CT angiography: a report of the Society of Cardiovascular Computed Tomography Guidelines Committee. J Cardiovasc Comput Tomogr 2014;8:342-58.

79. Raff GL, Abidov A, Achenbach S, et al. SCCT guidelines for the interpretation and reporting of coronary computed tomographic angiography. J Cardiovasc Comput Tomogr 2009;3:122-36.